

RAPID COMMUNICATIONS

Rapid Communications are intended for the accelerated publication of important new results and are therefore given priority treatment both in the editorial office and in production. A Rapid Communication in Physical Review B may be no longer than four printed pages and must be accompanied by an abstract. Page proofs are sent to authors.

Kinetics of metal-catalyzed growth of single-walled carbon nanotubes

A. Maiti

Solid State Division, Oak Ridge National Laboratory, Oak Ridge, Tennessee 37831

C. J. Brabec and J. Bernholc

Department of Physics, North Carolina State University, Raleigh, North Carolina 27695

(Received 21 November 1996)

Molecular-dynamics and total-energy calculations using a realistic three-body potential for carbon reveal the basic atomic processes by which single-shelled nanotubes can grow out of metal-carbide particles by the root growth mechanism. We find that nanometer-sized protrusions on the metal-particle surface lead to the nucleation of very narrow tubes. Wide bumps lead to a strained graphene sheet and no nanotube growth. The results also explain the absence of multishelled tubes in metal-catalyzed growth. [S0163-1829(97)51210-0]

The syntheses of single-walled graphitic tubes (SWT's) in the presence of Fe (Ref. 1) and Co (Ref. 2) catalysts have instilled a new impetus into the study of carbon nanotubes. SWT's are expected to be much more free of defects than the multiwalled nanotubes synthesized previously.³ Not surprisingly, therefore, intense activities among many research groups have yielded successful synthesis of SWT's (Refs. 4–13) using many different catalysts: transition metals Fe, Co, Ni, and Cu, lanthanide metals Gd, Y, and La, as well as several mixed catalysts.^{7,10,13} Nanotubes produced in all the above experiments show a narrow dispersion in diameter, varying between 0.8 and 3.1 nm depending on the catalyst used, and the longest tubes grow up to a few μm .

Metal-catalytic growth of carbon nanotubes is widely believed to proceed via solvation of carbon vapor into metal clusters, followed by precipitation of excess carbon in the form of nanotubes. However, depending on the size of the metal particles involved, there are two different modes of catalytic growth of SWT's: (1) in which the metal particles, several tens of nm wide, are much larger than the tube diameters, and lead to the precipitation of a large number of SWT's from a single particle surface;^{8,9} and (2) in which the metal particles are of the same size or even smaller than the tube diameters (~ 1 nm) and prevent tube closure by moving with the growing tip.^{13–15} SWT growth by mode (2), when it occurs, is relatively simple, and is explained by the presence

of reactive dangling bonds at the tube tip.^{13–15} The dangling bonds are stabilized by the metal particles, and act as attraction sites for carbon adatoms.

However, mode (1), which implies *root growth* by carbon atoms precipitating from large metal particles, occurs in most experiments. This is because almost all SWT's are extracted from a weblike material consisting of rounded soot particles, several tens of nm in size.² The soot particles have been identified as metal clusters embedded in a few layers of graphitic carbon, which are interconnected by SWT's, several μm in length. Another direct evidence in support of root growth is that the use of lanthanide series catalysts (Gd, Y, La) yields a morphology^{5,8,10} in which a dense bundle of SWT's emanates radially from each metal particle. The main challenges associated with growth mode (1) are to understand (i) what limits the width of all SWT's to within ~ 3 nm, while precipitating from a metal-carbide particle of size several tens of nm; and (ii) what prevents the formation of multishelled tubes. It should be mentioned here that an alternative to root growth mechanism, which involves carbon atoms diffusing along the tube stem and attaching to the open tip, has recently been suggested.¹⁴ However, such a mechanism must be accompanied by a direct condensation of carbon atoms from the vapor phase onto the growing stem of the tube. Otherwise, the growth rate is too slow to account for the observed growth of SWT's to several hundreds of

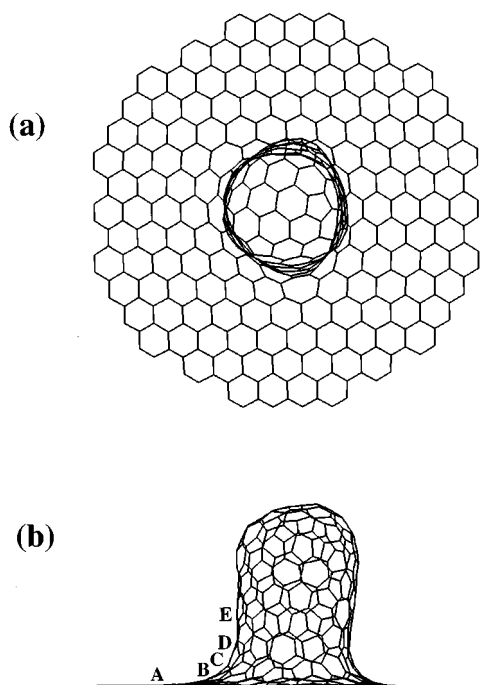


FIG. 1. The initial geometry for MD simulations of nanotube growth. A nanotube of helicity (11, 3) (diameter 1.0 nm) grows out of a flat all-hexagonal graphene sheet. (a) Top view; (b) side view. The side view also displays sites where handle energies are listed in Table I.

microns,¹⁴ as shown by estimates from a simple random-walk model.¹⁶

In this paper, we use molecular-dynamics simulations and total-energy calculations in order to analyze growth mode (1). In the process, we reveal the atomistic picture of growth of the SWT's. This includes carbon atoms precipitating from the metal particle, migrating to the tube base, and depositing a net number of hexagons to the tube stem, thereby leading to defect-free growth. The root growth mechanism, discussed here, is to be sharply contrasted with the growth at open-ended tips.^{14,15} In the latter case, a large number of dangling bonds are already present, leading to tremendous kinetic flexibility.

The simulation geometry consists of a large metal particle, embedded in a graphene sheet, out of which a close-capped single-shelled nanotube protrudes (Fig. 1). The graphene sheet represents the outermost layer of graphitic material encasing the metal particle in actual experiments.⁹ Most of our simulations are performed on a tube of helicity (11, 3) (diameter 1.0 nm). As in our previous work,^{15,17} the Tersoff-Brenner potential¹⁸ is used to model the interatomic potential for carbon, and the equations of motion are integrated by a fifth-order Beeman-Verlet algorithm using a time step of 0.5 fs. A simulation temperature of 2000 K, higher than actual experimental values of ~ 1000 K, is maintained by renormalizing the total kinetic energy every 2500 time steps. The high simulation temperature is mandated by the kinetic processes of interest, which at experimental temperatures occur on a time scale much longer than the total simulation time.

Relevant to the simulations are the constraints imposed by Euler's theorem on the ring structure. In all simulations we

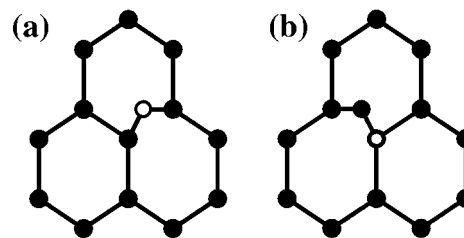


FIG. 2. Sketch of the atomistic mechanism of handle migration by the kick-out mechanism.

find that the only stable rings are hexagons, pentagons, and heptagons. Using this, and the fact that the geometry of Fig. 1 is topologically equivalent to a flat graphene sheet (net curvature=0), Euler's theorem implies that the total numbers of pentagons (n_5) and heptagons (n_7) in Fig. 1 are equal. Furthermore, for a tube that has grown a few layers, its base (root) and tip are separated by a well-defined stem. In such a case, Euler's theorem yields the following results: (a) at the base, $n_7 - n_5 = 6$; (b) at the tip, $n_5 - n_7 = 6$ (for a closed tip); and (c) at the stem, $n_5 = n_7 = 0$. Figure 1, for example, has the following initial values of (n_5 , n_7): (1, 7) at the base; (6, 0) at the tip; and (0, 0) on the stem. The aim of an atomistic theory of root growth is to delineate (i) how atoms precipitating from the metal particle, i.e., below the root, migrate to the tube base and lead to the addition of a net number of hexagons; and (ii) how the tube starts to grow, i.e., nucleates. We first address the question of hexagon addition.

For simplicity, we discuss the case where only carbon atoms precipitate from the metal particle, noting that dimers and trimers do not qualitatively change the growth picture described below. The first question is how the atoms precipitating from just below the all-hexagonal region away from the tube base get incorporated in the local hexagonal network. In all simulations we find the *unique* answer that a precipitated atom forms a *handle* between a pair of nearest-neighbor carbon atoms [Fig. 2(a)]. Thus each handle atom is twofold coordinated, flanked by threefold-coordinated carbon atoms which were nearest neighbors in the absence of the handle. In the terminology of the well-studied field of diffusion in semiconductors, the handle acts like an interstitial point defect, and imparts tremendous kinetic flexibility to the structure by being able to migrate thermally. As portrayed in Fig. 2(b), the migration mechanism involves a kick out by the handle atom of one of its two neighboring atoms. The kicked-out atom forms a new handle, while the previous handle atom becomes one of its threefold-coordinated neighbors. On a flat graphene sheet the handle does not have any preferential site and will thermally migrate on the hexagonal network until it reaches the tube base.

Table I lists the energetics of an atomic handle as a function of its location at and around the tube base. We find that the energy depends strongly on the local curvature of the surface, being the lowest at the point of the highest curvature [C in Fig. 1(b)]. This is precisely the region where the heptagons are located. The binding energy of the handle to this region is ~ 0.5 eV. Thus at experimental temperatures of less than 1000 K, when most of the SWT's precipitate, the handles are essentially confined to the high curvature region of the base. However, an isolated handle cannot lead to the

TABLE I. The energy of a single handle at various sites around the base of the nanotube (see Fig. 1).

Handle site	Energy
A	0.0
B	-0.1
C	-0.5
D	-0.2
E	0.05

addition of hexagons, for which one needs an even number of handles. Total energy calculations show that although the energy of an isolated handle depends only on the local curvature and not on the ring it is on, a pair of handles prefer to be on the opposite sides of a heptagon. This is because a heptagon can provide a larger separation between two handle atoms than a pentagon and a hexagon. Our molecular dynamics (MD) simulations demonstrate that the addition of hexagons occurs through a sequence of processes involving a pair of handles on the opposite bonds of a heptagon, as described below.

Figure 3 schematically displays the process of hexagon addition. Fig. 3(a) shows the particular case of an isolated heptagon (i.e., surrounded only by hexagons) supporting two handles on opposite bonds. A bond forming between these two handle atoms yields a fully trivalent structure in which the original heptagon is converted into a pentagon-hexagon pair and the two neighboring hexagons are each converted into a heptagon. In short, the original 6-7-6 structure is converted into a 7-5-7 structure, plus a hexagon. Thus, this process of hexagon generation also creates a 5-7 pair, which keeps Euler's condition satisfied at the base. The 5-7 pair merely creates a wiggle in the local topology, without alter-

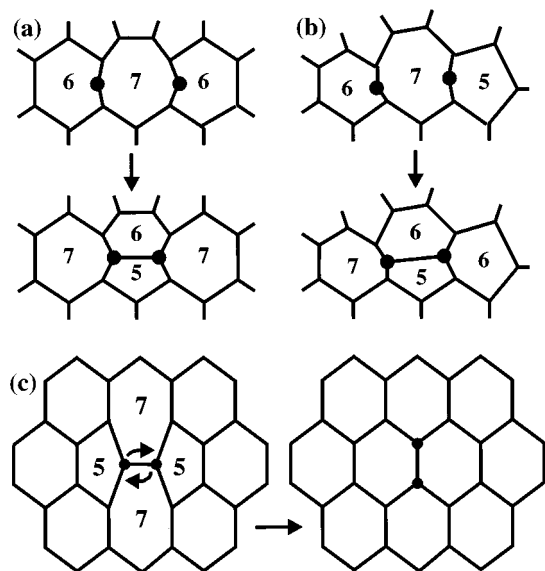


FIG. 3. The atomistics of hexagon addition at the nanotube base by bond formation between a pair of handle atoms at the opposite sides of a heptagon. (a) For an isolated heptagon, a 5-7 pair forms in addition to a hexagon; (b) for a 5-7-6 complex only an additional hexagon forms; (c) annihilation of two adjacent 5-7 pairs into four hexagons by a reverse Stone-Wales switch.

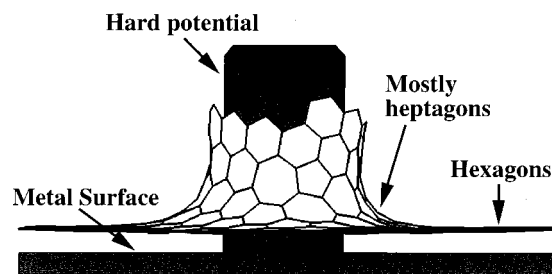


FIG. 4. A snapshot from a MD simulation for a narrow tube ($d_p \ll h$) showing curving up and growth.

ing the local curvature.¹⁹ Figure 3(b) shows a process in which a pair of handles on the heptagon of a 5-7 pair leads to the net addition of a hexagon, without creating another defect. Thus, after the formation of the first 5-7 pair, a pair of handles in the vicinity predominantly yields a net addition of hexagons only, thereby limiting the number of 5-7 defects at the base. The number of 5-7 pairs is also limited by processes of 5-7 annihilation into hexagons. For instance, in some of our MD simulations two adjacent 5-7 pairs generated by the process of Fig. 3(a) led to a 5-7-7-5 geometry of Fig. 3(c), which was converted into four hexagons by a reverse Stone-Wales bond switch²⁰⁻²² within a few ps. Such a process is expected to be even more efficient in the presence of extra carbon atoms²³ in the form of handles. Thus, a long enough growth process is expected to yield a limited number of 5-7 pairs in equilibrium with six additional heptagons at the tube base, while there is a constant addition of hexagons to the bottom of the tube stem.

Providing an atomistic picture of nanotube nucleation is more difficult. The chemical processes involved in coevaporation of carbon and metal in the arc discharge, the solvation of carbon into metal in the vapor phase, condensation of metal-carbide particles into quasispherical droplets upon cooling, and subsequent precipitation of carbon, are extremely complex. Simulating all these steps requires a microscopically detailed understanding of the process of arc discharge evaporation, as well as an accurate potential describing the interaction of carbon with the metal atoms, none of which are presently available. We have therefore combined MD simulations on the carbon system with a simple *conjecture* on the topology of the metal-particle surface, as described below.

TEM images of metal particles show a high degree of regularity in shape. This implies that the irregularities or undulations on the metal-particle surface are small compared to the particle diameter, which is of the order of a few tens of nm. Therefore, we make the conjecture that the metal-particle surface contains protrusions whose maximum height h is within a few nm. From MD simulations, described below, the following picture emerges: protrusions with diameter d_p small compared to h can lead to a SWT nucleation, while wider protrusions lead only to a strained graphene sheet and no nanotube growth.

Figure 4 shows a snapshot from our MD simulation for the case $d_p \ll h$, with the interaction between the precipitated carbon atoms and the carbon saturated metal particle being modeled by a cylindrically symmetric hard repulsive potential.¹⁵ The initial geometry consists of a hole of diam-

eter slightly larger than h . After a few ns simulation, the carbon atoms originally precipitated in the all-hexagonal region migrate in the form of handles to the edge of the initial hole, leading to the formation of heptagons and 7-5-7 structures that result in a geometry curving upwards (Fig. 4). This is the beginning stage of the formation of a SWT. Since the angle of contact of the protrusion with the metal surface is large, the curvature at the base of the protrusion is high. Therefore, handles migrating to this region get confined (see the energetics in Table I), and form hexagons by the mechanism described earlier. This results in the growth of an all-hexagonal stem. In our simulation the tube tip is kept open by the protrusion, but it is likely that the tip closes once it grows past the protrusion, in order to eliminate dangling bonds at the tube tip. A full MD simulation of this entire process would be prohibitively expensive at present.

We have also performed MD simulations of growth for the case $d_p > h$. As in the experiment described in the previous paragraph, atomic handles originating from a region away from the hole migrate to the edge of the hole and form pentagons and heptagons. However, unlike the previous case, the angle of contact of the protrusion with the metal surface is small. Thus, handles do *not* get confined to the base region of the protrusion, and the resulting pentagons or heptagons are uniformly distributed all over the tip of the protrusion. This leads only to a strained graphene sheet and no nanotube growth.

The above discussion would explain why all observed SWT's are narrow. The increased production of SWT's with specific mixed catalysts^{7,10,13} may be attributed to either (i) an enhancement in the precipitation of carbon atoms, (ii) changes in the activation barrier for growth, or (iii) the formation of a larger number of narrow protrusions.

Finally, our MD simulations also explain why multi-

shelled tubes do not form. In order to start a second shell, it is first necessary to nucleate a new graphene layer on the top of the existing outermost layer. This necessitates a cooperative phenomenon involving many handles in the all-hexagonal part, where the handles are freely migrating. In general, this would require times much longer than those in which individual handles migrate to the nearest tube base, get confined, and in combination with another handle get incorporated into the existing tube. The situation here is different from the growth of multishelled tubes on the cathode of a carbon arc discharge apparatus.²⁴ In the latter, the cathode surface is not necessarily oriented parallel to a single basal plane of graphite, and much higher arc temperatures produce a significantly larger number of defects on the cathode surface. Furthermore, the carbon flux, arriving from the tip side of the tube(s) is much higher.

In summary, MD simulations have revealed the basic atomic processes by which root growth of SWT's can occur from a metal-carbide surface. We find that adatoms form "handles" that are energetically attracted to the tube base. An even number of handles leads to an increase in the net number of hexagons, and thus to root growth. Under the assumption that the metal surface contains protrusions of height $h \sim$ a few nm, MD simulations yield the following picture: protrusions much narrower than h can nucleate and grow SWT's, while wider ones form only a strained graphene sheet and do not lead to tube growth. Our results explain why only very narrow SWT's are observed experimentally, and why multishelled tubes growing out of metal particles are not found.

This work was supported in part by the Office of Naval Research Grant No. N00014-91-J-1516.

-
- ¹S. Iijima and T. Ichihashi, *Nature (London)* **363**, 603 (1993).
²D. S. Bethune, C. H. Kiang, M. S. de Vries, G. Gorman, R. Savoy, J. Vasquez, and R. Beyers, *Nature (London)* **363**, 605 (1993).
³S. Iijima, *Nature (London)* **354**, 56 (1991); T. W. Ebbesen and P. M. Ajayan, *ibid.* **358**, 220 (1992).
⁴Y. Saito, T. Yoshikawa, M. Okuda, M. Fujimoto, K. Symiyama, K. Suzuki, A. Kasuya, and Y. Nishina, *J. Phys. Chem. Solids* **54**, 1849 (1993).
⁵S. Subramoney, R. S. Ruoff, D. C. Lorents, and R. Malhotra, *Nature (London)* **366**, 637 (1993).
⁶X. Lin, X. K. Wang, V. P. Dravid, R. P. H. Chang, and J. B. Ketterson, *Appl. Phys. Lett.* **64**, 181 (1994).
⁷S. Seraphin and D. Zhou, *Appl. Phys. Lett.* **64**, 2087 (1994).
⁸D. Zhou, S. Seraphin, and S. Wang, *Appl. Phys. Lett.* **65**, 1593 (1994).
⁹Y. Saito, M. Okuda, N. Fujimoto, T. Yoshikawa, M. Tomita, and T. Hayashi, *Jpn. J. Appl. Phys.* **1** **33**, L-526 (1994).
¹⁰Y. Saito, in *Recent Advances in the Chemistry and Physics of Fullerenes and Related Materials*, edited by K. M. Kadish and R. S. Ruoff (ECS, Pennington, 1994), p. 1419.
¹¹J. M. Lambert, P. M. Ajayan, P. Bernier, J. M. Planeix, V. Brotons, B. Coq, and J. Castaing, *Chem. Phys. Lett.* **226**, 364 (1994).
¹²Y. Saito, M. Okuda, M. Tomita, and T. Hayashi, *Chem. Phys. Lett.* **236**, 419 (1995).
¹³T. Guo, P. Nikolaev, A. Thess, D. T. Colbert, and R. E. Smalley, *Chem. Phys. Lett.* **243**, 49 (1995).
¹⁴A. Thess *et al.*, *Science* **273**, 483 (1996).
¹⁵A. Maiti, C. Brabec, C. Roland, and J. Bernholc, *Phys. Rev. B* **52**, 14 850 (1995).
¹⁶A. Maiti (unpublished).
¹⁷C. Brabec, A. Maiti, C. Roland, and J. Bernholc, *Chem. Phys. Lett.* **236**, 150 (1995).
¹⁸D. W. Brenner, in *Atomic Scale Calculations in Materials Science*, edited by J. Tersoff, D. Vanderbilt, and V. Vitek, MRS Symposia Proceedings No. 141 (Materials Research Society, Pittsburgh, 1989), p. 59; *Phys. Rev. B* **42**, 9458 (1990).
¹⁹C. J. Brabec, A. Maiti, and J. Bernholc, *Chem. Phys. Lett.* **219**, 473 (1994).
²⁰A. J. Stone and D. J. Wales, *Chem. Phys. Lett.* **128**, 501 (1986).
²¹J.-Y. Yi and J. Bernholc, *J. Chem. Phys.* **96**, 8634 (1992).
²²G. E. Scuseria, *Science* **271**, 942 (1996).
²³B. R. Eggen, M. I. Heggie, G. Jungnickel, C. D. Latham, R. Jones, and P. R. Briddon, *Science* **272**, 87 (1996).
²⁴S. Iijima, *Nature (London)* **354**, 56 (1991).